Electrochimica Acta 460 (2023) 142618

Contents lists available at ScienceDirect

Electrochimica Acta

journal homepage: www.journals.elsevier.com/electrochimica-acta

# A single-step enzyme-free electrochemical assay of *N*-acetyl-D-neuraminic acid

Saurav K. Guin [a,*], Tobias Krämer [a,c], Eithne Dempsey [a,b,*]

[a] Department of Chemistry, Maynooth University, Maynooth, Co. Kildare, Ireland
[b] Kathleen Lonsdale Institute for Human Health, Maynooth University, Maynooth, Co. Kildare, Ireland
[c] Hamilton Institute, Maynooth University, Maynooth, Co. Kildare, Ireland

ARTICLE INFO

*Keywords:*
Voltammetry
Sialic acid
Neu5Ac
Rapid assay
Density functional theory

ABSTRACT

*N*-acetyl-D-neuraminic acid (Neu5Ac) is a sialic acid endogenously produced in higher vertebrates including humans. Its significant physiological, nutritional and clinical importance have been revealed over the past decades and recently European Commission has approved its regulatory inclusion as a nutrition additive in commercial food products. Therefore, assay of Neu5Ac in various types of samples has potential interest. However, the state of the art of Neu5Ac assay is suffering from complex-multistep methods, costly biochemicals, sophisticated expensive instruments or long analysis time. This work presents a proof of concept for developing a single-step, robust and economic electrochemical method based on a chemoreceptor *viz.* ferroceneboronic acid (FcBA) for rapid assay of Neu5Ac in the linear dynamic range 0.1-5.5 mM with a limit of detection up to 30 μM avoiding interference from other saccharides. Density functional theory calculations provided a valuable insight into the most thermodynamically stable geometry of the FcBA-Neu5Ac complex and its higher stability relative to the corresponding FcBA complexes of diol *viz.* glucose and $\alpha$-hydroxy acid *viz.* lactic acid.

## 1. Introduction

The nonulosonic acid monosaccharide *N*-acetyl-D-neuraminic acid (Neu5Ac) is an important member in the family of sialic acids. It is endogenously produced in higher vertebrates and it participates in a variety of physio- and pathological activities in humans [1–3]. It is now evident that Neu5Ac present in human milk is not only responsible for the neurocognitive development of the human brain and alteration of gut-microbiota of gut-brain axis at an early stage of life, but it also participates in a neuroprotective mechanism for some neurodegenerative diseases at later stages of life [4–6]. The concentration of total Neu5Ac in human milk in the colostrum, transition, one and three month(s) maturity stages for full-term (pre-term) groups of mothers was reported as 5.04 ± 0.21 (5.76 ± 0.19), 3.46 ± 0.14 (4.27 ± 0.24), 1.98 ± 0.08 (2.56 ± 0.15) and 1.04 ± 0.06 (1.30 ± 0.13) mM, respectively [7], which depends on the pre-pregnancy body-mass-index, maternal age and mode of delivery [8], but may not be affected by mother's diet [9]. Commercial pre-term (0.63 ± 0.12 mM) and follow-on (0.43 ± 0.03 mM) infant formulas are unable to meet that level of Neu5Ac [7]. Thus, the European Commission has recently approved the regulatory inclusion of Neu5Ac·$2H_2O$ in commercial food products as a nutrition additive [10].

On the other hand, Neu5Ac contributes to the acidity of zona-pellucida and controls the oocyte maturation process. A positive correlation between the follicular fluid total Neu5Ac (~2.8 mM) and immature oocytes has been found during *in vitro* fertilisation studies [11]. The total serum Neu5Ac (~0.8 mM) is a potential postnatal biomarker for acute placental inflammatory lesions and is useful to predict the severity of intrauterine infection in preterm infants [12]. It also takes part in the glycan mediated B-cell suppression establishing fetomaternal tolerance and enables antibody protection against intracellular infection.[13,14] It is also a potential biomarker for the diagnosis and risk stratification of acute coronary syndrome [15], and development of tumours [16].

Therefore, the assay of Neu5Ac in commercial food, biological and clinical matrices is of interest. It is evident from a state of the art review [1] and some latest reports [16–19], that most of the assay methods rely on either expensive multiple enzymes, unstable fluorophore tag molecules, multi-step biochemical procedures or sophisticated equipment such as high performance liquid chromatography mass spectrometry and multiple sample preparation steps followed by sufficiently long analysis time (>2 h). On the other hand, the commercially available assay kits based on the multi-step enzymatic reactions or periodate

* Corresponding authors at: Department of Chemistry, Maynooth University, Maynooth, Co. Kildare, Ireland.
*E-mail addresses:* sauravkrguin@yahoo.co.in, sauravkumar.guin@mu.ie (S.K. Guin), eithne.dempsey@mu.ie (E. Dempsey).

https://doi.org/10.1016/j.electacta.2023.142618
Received 9 March 2023; Received in revised form 17 May 2023; Accepted 18 May 2023
Available online 19 May 2023

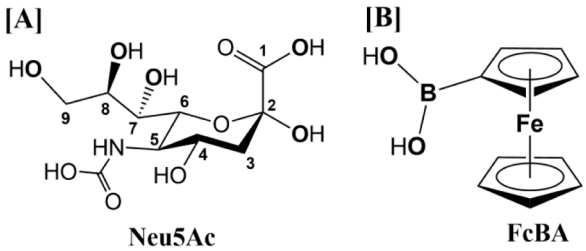


**Fig. 1.** The molecular structure of [A] *N*-acetyl-D-neuraminic acid (Neu5Ac) and [B] ferroceneboronic acid (FcBA).

oxidation followed by colourimetric/fluorometric measurements can produce a linear dynamic range (LDR) of 0.02/0.005-1.0 mM by colourimetry and 0.005/0.0005-0.100 mM by fluorimetry methods with minimum 60 min assay time [1]. This LDR is insufficient for the assay of Neu5Ac in the cases discussed above.

Neu5Ac has both diol functional group at C-7/8,9 and α-hydroxy carboxylic acid functional group at C-1,2 as shown in Fig. 1[A]. Thus Neu5Ac has shown a special chemical affinity towards various boronic acid functionalised molecules [1]. Hence, a boronic acid functional group containing redox molecule was thought to be a suitable redox probe as well as chemoreceptor of Neu5Ac and from this perspective ferroceneboronic acid (FcBA) (Fig. 1B) was proposed as the most promising redox active chemoreceptor for Neu5Ac towards the objective of this study.

It is well known that FcBA and other boronic acids form stable boronate ester(s) (E) with the ligand (L) in the form of both di-/poly-ol [20–30,30–47] or α-hydroxy carboxylic acid [48] by following the reaction as shown in Scheme 1. The saccharides and α-hydroxy acids are not electroactive in water, but possess diol and hydroxy-acid functional groups, respectively, which can form boronate esters with either $sp^2$ (*i.e.*, $-B(OH)_2$) or $sp^3$ (*i.e.*, $-\overline{B}(OH)_3$) hybridised boron (B) of a boronic acid functional group anchored to an electroactive molecule such as FcBA, although sugars and α-hydroxy acids show different chemical affinities to boronic acid.[1,33,42].

However, to the best of our knowledge, no electrochemical study of FcBA with Neu5Ac is reported in the literature considering the question of selectivity of this important nonulosonic acid compared to other sugars. Hence, this work has the ambition to present a proof of concept to develop a single-step, robust, economic and rapid electroanalytical assay of Neu5Ac even in the presence of biologically and commercially relevant sugars and sugar alcohols.

## 2. Experimental

### 2.1. Materials

Ferroceneboronic acid (FcBA), *N*-acetyl-D-neuraminic acid (Neu5Ac), *N*-glycolyl-D-neuraminic acid (Neu5Gc), D(+)-glucose, D(-)-fructose, D(+)-galactose, D(+)-xylose, maltose, sucrose, lactose, D(-)-xylitol, D(-)-mannitol, D(-)-sorbitol, sodium L(+)-lactate, bovine serum albumin (BSA), anhydrous sodium acetate and glacial acetic acid of analytical grades were used in this work without any further treatment. All aqueous solutions were prepared with ultrapure Milli-Q Millipore water (18.2 MΩ cm).

### 2.2. Electrochemical experiments

The cyclic and square wave voltammetry experiments were carried out at room temperature (22 ± 2 °C) in an electrochemical glass cell consisting of a glassy carbon working electrode of diameter 3 mm (CHI104), platinum wire counter electrode (CHI115) and Ag/AgCl(3M KCl) reference electrode (CHI111) by using CHI660E electrochemical workstation. Before and between the electrochemical experiments, the working electrode was polished on a polishing pad containing slurry of 1 μm monocrystalline diamond suspension and thoroughly washed with Millipore water and 5 mL of test solutions were purged with high purity nitrogen for 10 min. Electrochemical experiments were carried out in triplicate and a very stable and robust electrochemical response was recorded from the same electrode for months. The pH of the solution was measured by a calibrated Jenway 550 pH meter.

### 2.3. Computational methods

All geometry optimisations were carried out with the ORCA 5.0.2 program package [49]. All calculations utilised the second-order Douglas-Kroll-Hess Hamiltonian to incorporate scalar relativistic effects [50–52]. The compounds were optimised at the DFT level of theory using the TPSSh functional with D3(BJ) dispersion corrections and the DKH-def2-TZVP(–f) basis set on all atoms [53–59]. Tight convergence and optimisation criteria (TightSCF, TightOpt) and a finer grid (defgrid3) were used. To speed up the calculations the RIJCOSX approximation was used in conjunction with the SARC/J fitting basis set [60–65]. Thermal and entropic corrections ($T = 298.15$ K, $p = 1.00$ atm) to the energy were obtained from calculation of the analytical Hessian matrix. Final single point energies were calculated on the optimised geometries and by replacing the above basis set by the larger dhk-def2-tzvpp basis set. The effect of bulk solvent (water) was

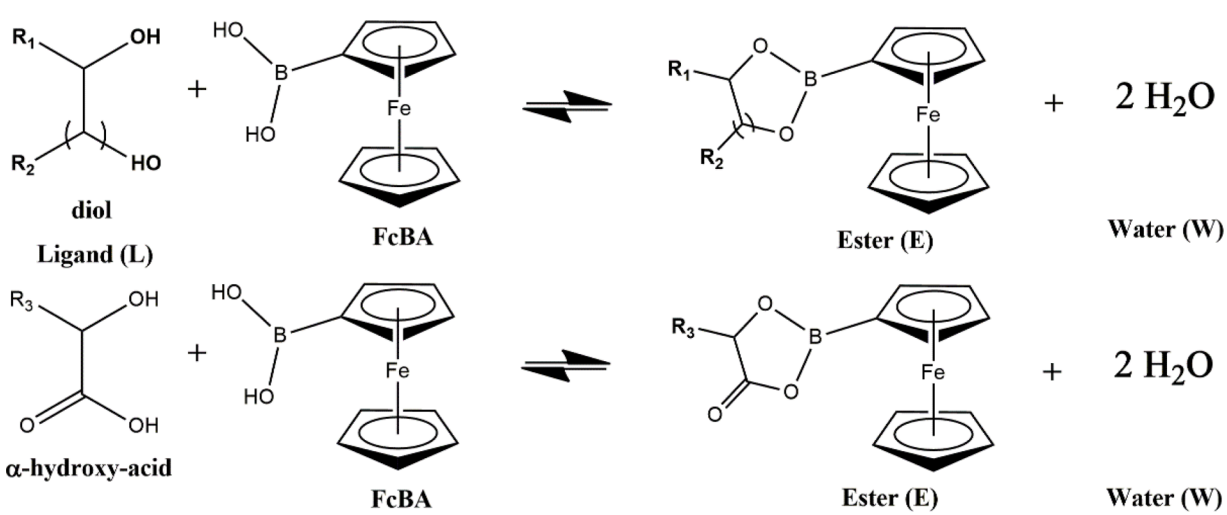


**Scheme 1.** The esterification reaction between the L (di-/poly-ol or α-hydroxy acid) and FcBA.

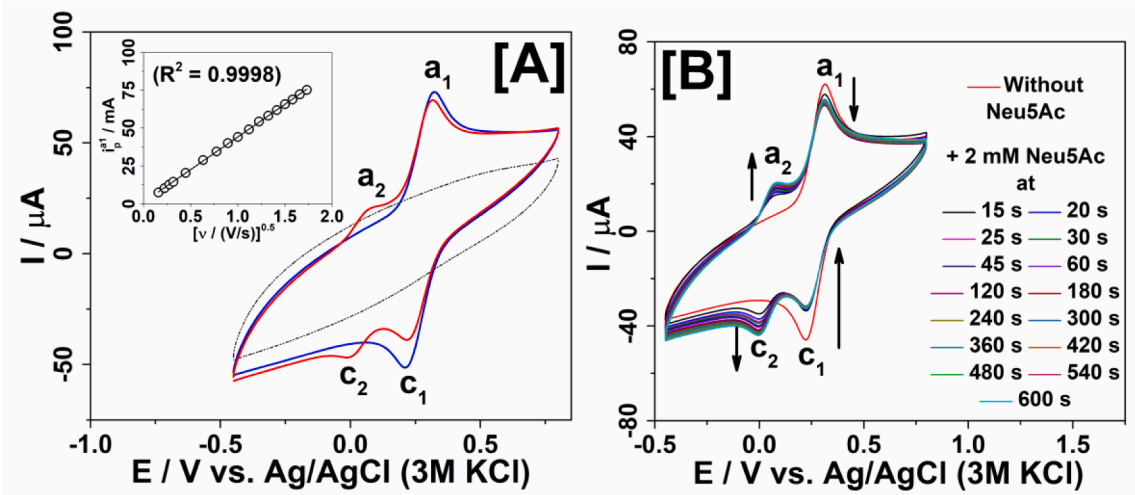


**Fig. 2.** CVs of 0.1 M acetate buffer (pH 4.5) (dotted line), 1 mM FcBA in 0.1 M acetate buffer (pH 4.5) in the absence (blue line) and presence (red line) of 2 mM Neu5Ac on glassy carbon electrode at $\nu = 1.000$ V s$^{-1}$. Inset: $i_p^{a1}$ vs. $\nu^{0.5}$ for $\nu = 0.025$-3.000 V s$^{-1}$. [B] CVs of 1 mM FcBA in 0.1 M acetate buffer (pH 4.5) recorded before and after adding 2 mM Neu5Ac at different time of incubation; $\nu = 1.000$ V s$^{-1}$.

modelled using the conductor-like polarizable continuum model (CPCM) in combination with the SMD approximation [66]. The initial guess structures were prepared and the optimised structures were analysed by using ChemCraft 1.8 software [67]. The Gibbs Free Energy of formation ($\Delta G_f$) of ester as shown in Scheme 1 was calculated from the Free Energy ($G$) of the solvated ester ($G_E$), water ($G_W$), FcBA ($G_{FcBA}$) and ligand ($G_L$) (as listed in Table S3) by the following equation (Eq. 1):

$$\Delta G_f = G_E + 2G_W - G_{FcBA} - G_L \quad (1)$$

## 3. Results and discussion

Fig. 2A shows the cyclic voltammograms (CVs) of 1 mM FcBA in 0.1 M acetate buffer (pH 4.5) in the absence (blue line) and presence (red line) of 2 mM Neu5Ac on a glassy carbon electrode at a scan rate ($\nu$) of 1.000 V s$^{-1}$. FcBA showed anodic and cathodic peak current of 44.1 μA ($I_p^{a1}$) at 0.323 V ($E_p^{a1}$) and -45.1 μA ($I_p^{c1}$) at 0.210 V ($E_p^{c1}$), respectively. In the presence of 2 mM Neu5Ac under similar condition, $I_p^{a1}$ and $I_p^{c1}$ were decreased to 35.5 μA and -33.6 μA, respectively, although $E_p^{a1}$ and $E_p^{c1}$ did not change. Furthermore, an additional pair of anodic and cathodic peak current of 6.9 μA ($I_p^{a2}$) at 0.064 V ($E_p^{a2}$) and -22.2 μA ($I_p^{c2}$) at -0.015 V ($E_p^{c2}$), respectively, appeared as a redox representation of FcBA-Neu5Ac ester. The diffusion coefficient of FcBA in 0.1 M acetate buffer (pH 4.5) was calculated as $5.3 \times 10^{-6}$ cm$^2$ s$^{-1}$ from the slope of the plot of $I_p^{a1}$ vs. $\nu^{0.5}$ (Inset of Fig. 2A) by using the Randles–Sevcik equation and all the CVs for $\nu = 0.025$-3.000 V s$^{-1}$ are shown in Fig. S1A-C. The log($I_p^{a1}$ or $I_p^{c1}$) vs. log($\nu$) plots showed straight lines of slope 0.49 or 0.41 and 0.46 or 0.51 in the absence and presence of Neu5Ac, respectively (Fig. S1D) indicating an electrochemical reaction controlled by diffusion controlled mass transfer to the electrode (theoretically it should be 0.5). However, log($I_p^{a2}$ or $I_p^{c2}$r) vs. log($\nu$) plots showed straight lines of slope 0.97 (up to 1.000 V s$^{-1}$) or 0.27 (>1.000 V s$^{-1}$) due to the change of the shapes of CVs at high $\nu$ (Fig. S1E). The shape of peak $a_2$ became more prominent at high $\nu$ (with little change >1000 V s$^{-1}$) where a reverse trend was observed for peak $c_2$, however $E_p^{a1}$, $E_p^{c1}$, $E_p^{a2}$, and $E_p^{c2}$ did not have noticeable change with $\nu$ (Fig. S1F). The formal reduction potential ($E_0^{'}$) of FcBA in the absence ($E_0^{'(1)}$) and presence ($E_0^{'(1)}$) of Neu5Ac was calculated as 0.267 ± 0.002 V and 0.265 ± 0.006 V, respectively, whereas that of FcBA-Neu5Ac ester ($E_0^{'(2)}$) was calculated as 0.027 ± 0.005 V. The shift of $E_0^{'}$ of FcBA-Neu5Ac to a less positive value

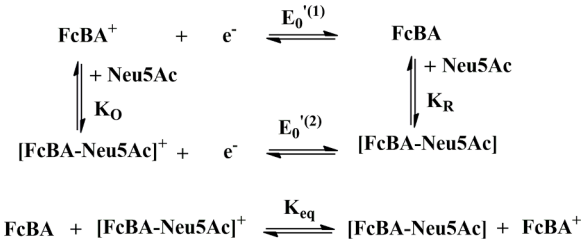


**Scheme 2.** The square scheme mechanism of the electrochemical and chemical reactions of FcBA and Neu5Ac. The molecule of water is not considered here as the reaction happened in an aqueous solution of FcBA and Neu5Ac.

compared to FcBA indicated that the Neu5Ac boronate ester group provided more electron density to the electroactive iron metal centre compared to the free boronic acid functionality. Fig. 2B shows that the formation of the FcBA-Neu5Ac ester in 0.1 M acetate buffer (pH 4.5) was very fast such that signal stability was achieved within 300 s from the time of addition of 2 mM Neu5Ac in 1 mM FcBA. However, to get more reliable data, we provided a minimum 600 s of incubation period for all experiments.

The above mentioned observations could be explained by a square-scheme reaction as shown in Scheme 2. [31]. The equilibrium constant of the chemical reaction of Neu5Ac in the oxidised and reduced form of FcBA are represented by $K_O$ and $K_R$, respectively Eqs. (2) and (3). The equilibrium constant of the overall chemical reaction is $K_{eq}$ (Eq. (4).

$$\text{Hence; } K_O = \frac{[\text{FcBA} - \text{Neu5Ac}]^+_{eq}}{[\text{FcBA}]^+_{eq}[\text{Neu5Ac}]_{eq}} \quad (2)$$

$$K_R = \frac{[\text{FcBA} - \text{Neu5Ac}]_{eq}}{[\text{FcBA}]_{eq}[\text{Neu5Ac}]_{eq}} \quad (3)$$

$$K_{eq} = \frac{K_R}{K_O} = \exp\left[\frac{F}{RT}\left\{E_0^{'(1)} - E_0^{'(2)}\right\}\right] \quad (4)$$

From the experimental data as discussed above, the value of $K_{eq}$ was calculated as $1.15 \times 10^4$, which suggested that Neu5Ac preferred the complex formation with FcBA (*i.e.*, reduced form) compared to FcBA$^+$ (*i.e.*, oxidised form). Hence, the low value of $\frac{I_p^{a2}}{I_p^{c2}}$ (0.02 at $\nu = 0.025$ V s$^{-1}$ to 0.31 at $\nu = 1.000$ V s$^{-1}$ (as shown in Fig. S2) was attributed to the high

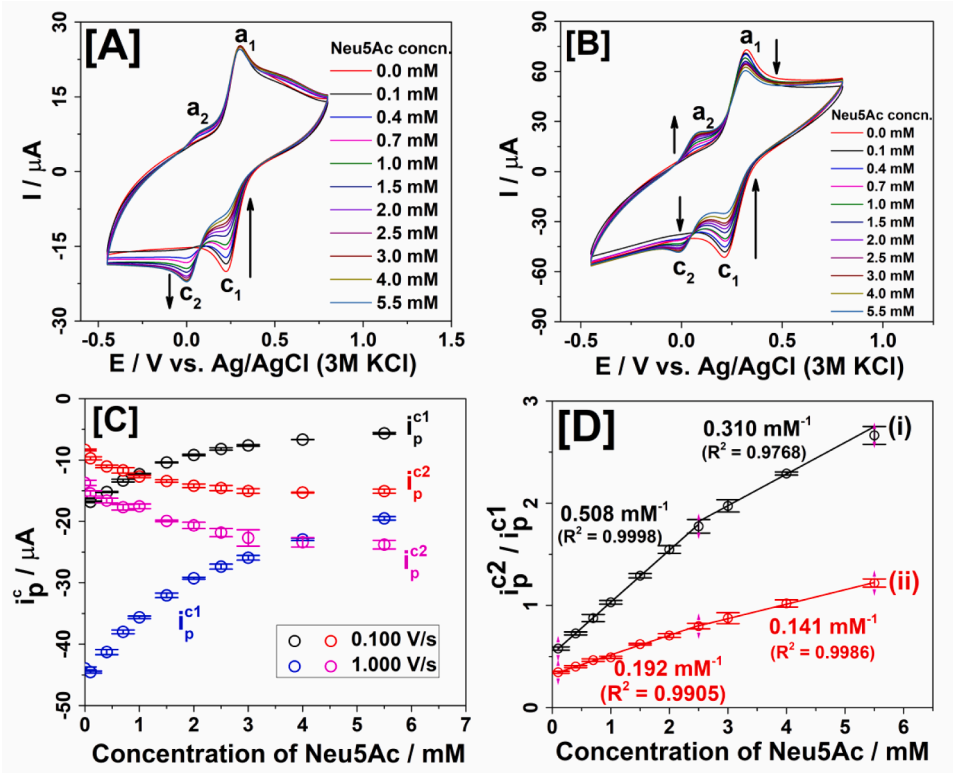


**Fig. 3.** CVs of 1 mM FcBA in 0.1 M acetate buffer (pH 4.5) in the absence and presence of 0.1-5.5 mM Neu5Ac on glassy carbon electrode at $\nu$ = [A] 0.100 and [B] 1.000 V $s^{-1}$. (C) $I_p^{c1}$ and $I_p^{c2}$ as a function of Neu5Ac concentration in 1 mM FcBA in 0.1 M acetate buffer (pH 4.5). [D] Plot of $i_p^{c2}/i_p^{c1}$ *vs.* concentration of Neu5Ac at $\nu$ = (i) 0.100 and (ii) 1.000 V $s^{-1}$.

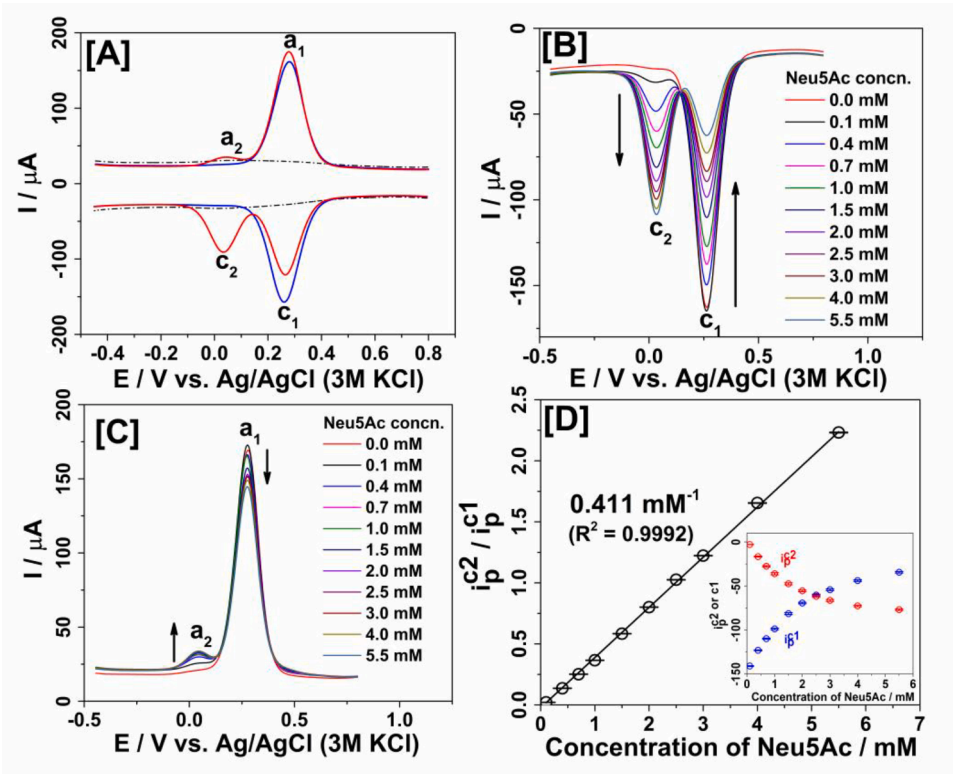


**Fig. 4.** [A] SWVs of 0.1 M acetate buffer (pH 4.5) (dotted line), 1 mM FcBA in 0.1 M acetate buffer (pH 4.5) in the absence (blue line) and presence (red line) of 2 mM Neu5Ac on glassy carbon electrode (f = 100 Hz, ΔE = 0.050 V). (B) Cathodic and (C) anodic SWVs of 1 mM FcBA in 0.1 M acetate buffer (pH 4.5) in the absence and presence of 0.1-5.5 mM Neu5Ac. (D) $i_p^{c2}/i_p^{c1}$ *vs.* Neu5Ac concentration. Inset: $i_p^{c1}$ and $i_p^{c2}$ vs. Neu5Ac concentration.

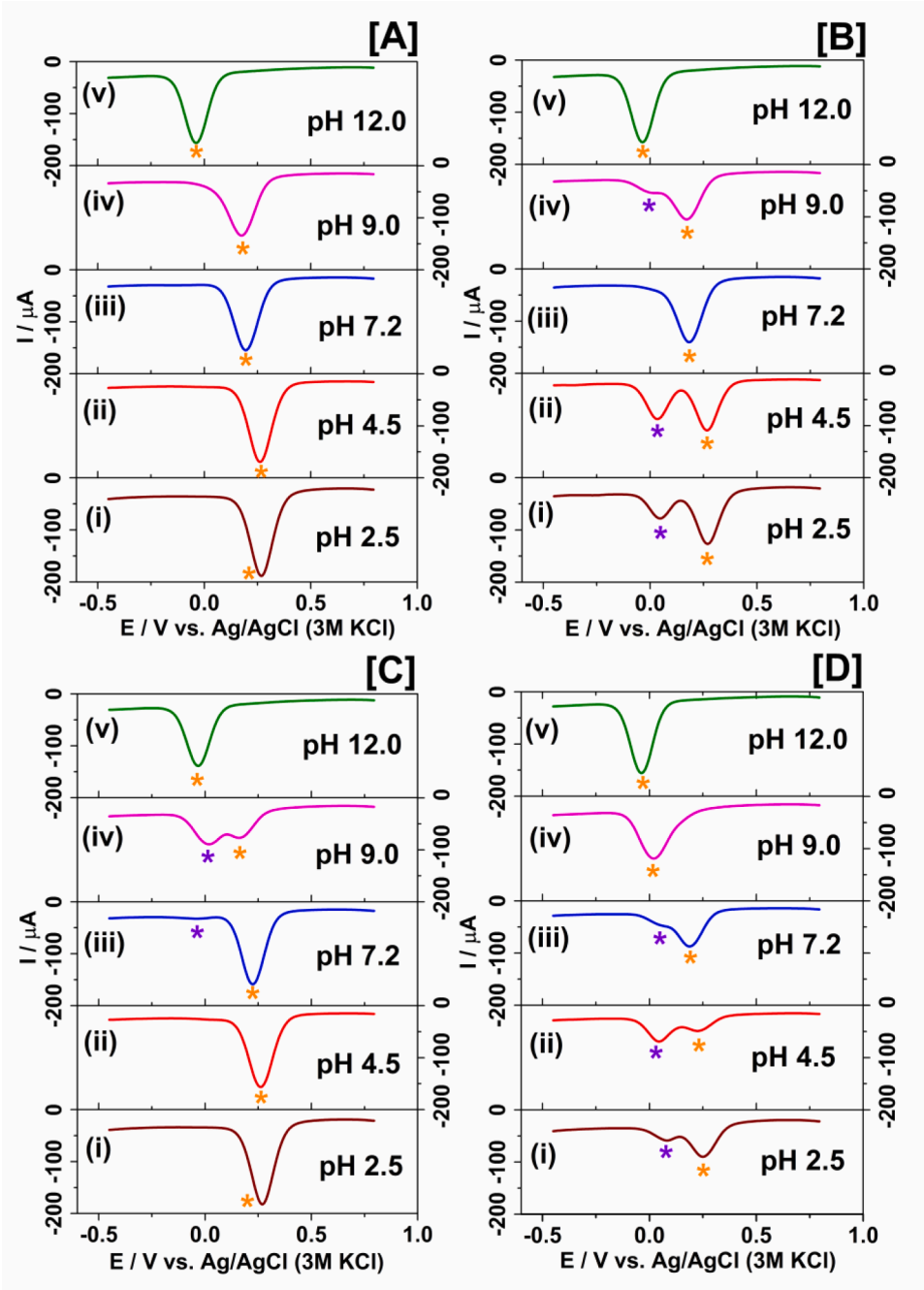


**Fig. 5.** Cathodic SWVs of 1 mM FcBA on glassy carbon electrode at pH (i) 2.5, (ii) 4.5, (iii) 7.2, (iv) 9.0 and (v) 12.0 in the absence (A) and presence of 2 mM Neu5Ac (B), 10 mM D(+)-glucose (C) and 10 mM L(+)-lactate (D). The peaks corresponding to free FcBA and FcBA ester are marked by orange and violet asterisk, respectively.

value of $K_{eq}$.

The CVs of 1 mM FcBA in the absence and presence of 0.1-5.5 mM Neu5Ac at $\nu = 0.100$ V $s^{-1}$ and 1.000 V $s^{-1}$ are shown in Fig. 3A and Fig. 3B, respectively. The $I_p^{c1}$ decreased, but $I_p^{c2}$ increased with increasing concentration of Neu5Ac for a fixed concentration of FcBA. The non-linear variation of $I_p^{c1}$ and $I_p^{c2}$ with Neu5Ac concentration is smaller in magnitude at 0.100 V $s^{-1}$ compared to that at 1.000 V $s^{-1}$. The $I_p^{c1}$ and $I_p^{c2}$ crossed over each other ~1 mM (for 0.100 V $s^{-1}$) and ~4 mM (for 1.000 V $s^{-1}$) of Neu5Ac (Fig. 3C). The ratiometric plot of $i_p^{c2}/i_p^{c1}$ *vs.* Neu5Ac concentration showed two linear dynamic ranges (Fig. 3D). The sensitivities 0.508 and 0.310 $mM^{-1}$ at 0.100 V $s^{-1}$ (i) was found to be higher compared to those 0.192 and 0.141 $mM^{-1}$ at 1.000 V $s^{-1}$ (ii). The limit of detection (LOD, S/N=3) and limit of quantification (LOQ, S/N=10) of Neu5Ac by CV at $\nu = 0.100$ V $s^{-1}$ were calculated as 0.05 and 0.17 mM, respectively.

The square wave voltammograms (SWVs) reflect a superior current sampling technique compared to CVs and thus was expected to show better electrochemical response for FcBA-Neu5Ac ester. Fig. 4A shows anodic and cathodic SWVs of 1 mM FcBA in 0.1 M acetate buffer (pH 4.5) in the absence (blue line) and presence (red line) of 2 mM Neu5Ac on a glassy carbon electrode. FcBA showed an anodic and cathodic peak current of 138.1 μA ($I_p^{a1}$) at 280 V ($E_p^{a1}$) and -133.5 μA ($I_p^{c1}$) at 0.260 V ($E_p^{c1}$), respectively. In the presence of 2 mM Neu5Ac, $I_p^{a1}$ and $I_p^{c1}$ were changed to 147.3 μA and -88.9 μA, respectively, although $E_p^{a1}$ and $E_p^{c1}$ did

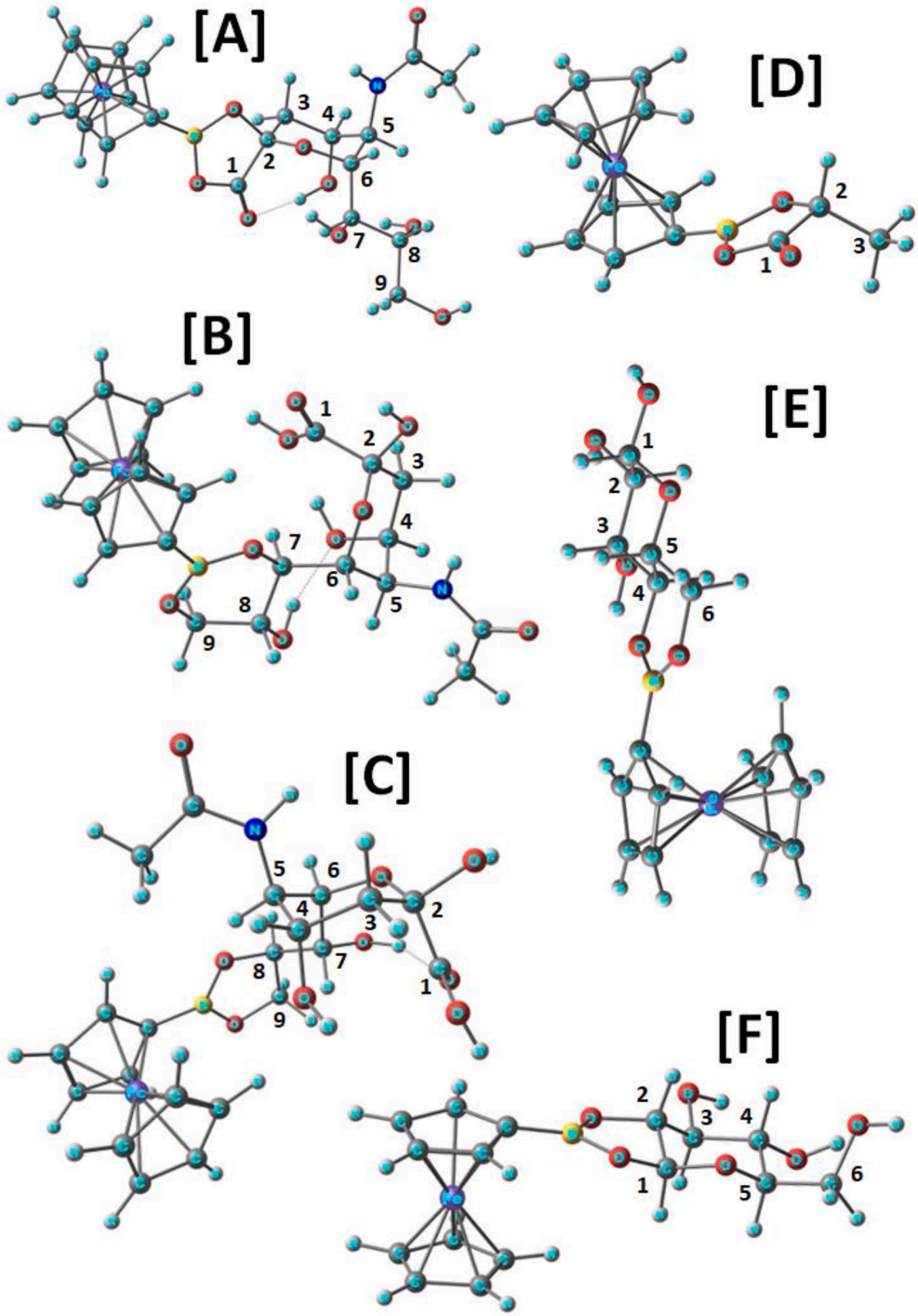


**Fig. 6.** Optimised molecular structures of (A) FcBA-1,2-β-Neu5Ac, (B) FcBA-7,9-β-Neu5Ac, (C) FcBA-8,9-β-Neu5Ac, (D) FcBA-1,2-L(+)-lactic acid, (E) FcBA-4,6-β-D(+)-glucose and (F) FcBA-1,2-β-D(+)-glucose in water as obtained by DFT calculation.

not change. The additional pair of anodic and cathodic peaks of 6.2 μA ($I_p^{a2}$) and -54.8 μA ($I_p^{c2}$) of FcBA-Neu5Ac ester appeared at 0.035 ($E_p^{a2}$) and 0.030 V ($E_p^{c2}$), respectively. The optimisation studies of the linear frequency (f) and potential pulse (ΔE) for SWVs (as shown in Fig. S3A-F) led us to use f = 100 Hz and ΔE = 0.050 V for SWV experiments to ensure good intensity and resolution of the peaks. The cathodic (Fig. 4B) and anodic (Fig. 4C) SWVs of FcBA in the absence and presence of 0.1-5.5 mM Neu5Ac revealed that the cathodic SWVs were much more sensitive and consistent for quantitative analysis of Neu5Ac. The $I_p^{c1}$ decreased, but $I_p^{c2}$ increased with increasing concentration of Neu5Ac and those crossed over at ~2.5 mM (Inset of Fig. 4D). The ratiometric plot of $I_p^{c2}/i_p^{c1}$ vs Neu5Ac concentration showed a single linear dynamic range of sensitivity, LOD and LOQ as 0.411 $mM^{-1}$, 0.03 and 0.11 mM, respectively (Fig. 4D).

Fig. 5A shows that cathodic peak of 1 mM FcBA $E_p^{c1}$ (marked by *) was shifted to more cathodic potentials at pH > 9.0 owing to the transformation of $sp^2$ hybridised B [*i.e.*, -$B(OH)_2$] to more electron rich $sp^3$ hybridised B [*i.e.* -$\overline{B}(OH)_3$] [31]. Fig. 5B shows that the cathodic peak of FcBA-Neu5Ac $E_p^{c2}$ (marked by *) only appeared at pH 2.5, 4.5 and 9.0. This indicates a pH sensitive boronate ester formation for

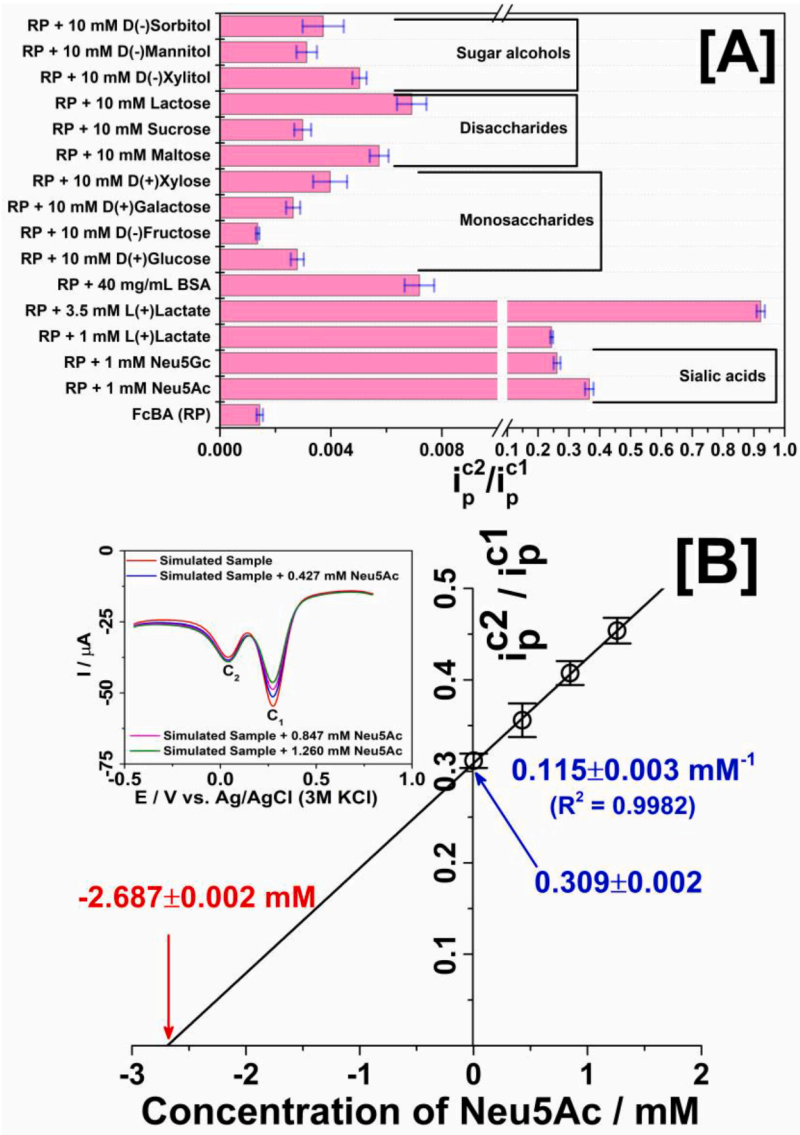


**Fig. 7.** [A] $I_p^{c2}/i_p^{c1}$ of cathodic SWV of 1 mM FcBA (redox probe, RP) in 0.1 M acetate buffer (pH 4.5) on glassy carbon electrode in the presence of selected interfering chemicals at specified concentrations. (B) Standard addition plot for recovery analysis of 2.5 mM (expected) Neu5Ac in 0.1 M acetate buffer (pH 4.5) containing 1 mM FcBA, 10 mM D(+)-glucose and 4% BSA. Inset: Corresponding cathodic SWVs.

Neu5Ac. Interestingly, the representative cathodic peak (marked by *) of the boronate ester of D(+)-glucose only appeared at pH 9.0 (Fig. 5C), but in contrast, the boronate ester of L(+)-lactate appeared only at pH 2.5, 4.5 and 7.2 (Fig. 5D). This clearly demonstrates that, depending on the pH of the aqueous solution, FcBA could form a boronate ester with either α-hydroxy carboxylic acid (at C-1,2) or diol (at C-7/8,9) functional unit of Neu5Ac, where the former was preferred at acidic pH. Fig. S4[A-D] shows the corresponding CVs at $\nu = 1.000$ V $s^{-1}$.

The thermodynamically stable structures of probable esters of FcBA with β-Neu5Ac, β-D(+)-glucose and L(+)-lactic acid in water were obtained by density functional theoretical (DFT) calculations and shown in Fig. 6A-F and the corresponding coordinates are listed in Table S2. A similar method was applied on (A) Neu5Ac, (B) D(+)-glucose, (C) L(+)-lactic acid, (D) FcBA and (E) water ($H_2O$) (Fig. S5; Table S1) to calculate Gibbs Free Energies ($G$) of individual optimised components and $\Delta G_f$ of esters by using Eq. (1) (Table S3). The $\Delta G_f$ decreased in the order FcBA-1,2-β-Neu5Ac (Fig. 6A) > FcBA-8,9-β-Neu5Ac (Fig. 6C) > FcBA-7,9-β-Neu5Ac (Fig. 6[B]) > FcBA-4,6-β-D(+)-glucose (Fig. 6E) > FcBA-1,2-L(+)-lactic acid (Fig. 6D); whereas the formation of FcBA-1,2-β-D(+)-glucose ester (Fig. 6F) was thermodynamically unfavourable (Table S3). It indicated that the planar 5-membered ring conformation in FcBA-1,2-β-Neu5Ac involving $sp^2$ hybridised C and B formed the most stable ($\Delta G_f$ = -64 kJ $mol^{-1}$) ester in water among the studied compounds. The thermodynamic stability of FcBA-1,2-β-Neu5Ac in water was higher compared to its α-hydroxy carboxylic acid analogue (FcBA-1,2-L(+)- lactic acid; $\Delta G_f$ = -21 kJ $mol^{-1}$). On the other hand, FcBA-8,9-β-Neu5Ac ($\Delta G_f$ = -58 kJ $mol^{-1}$) and FcBA-7,9-β-Neu5Ac ($\Delta G_f$ = -50 kJ $mol^{-1}$) were more thermodynamically stable in water compared to their diol analogue FcBA-4,6-β-D(+)-glucose ($\Delta G_f$ = -30 kJ $mol^{-1}$). Furthermore, the Mulliken atomic charge on iron became more negative for all esters compared to free FcBA (Table S3) and it justified the cathodic shift of $E_0^{'}$ of FcBA-esters relative to FcBA.

The $I_p^{c2}/i_p^{c1}$ of cathodic SWV of 1 mM FcBA (redox probe, RP) in 0.1 M acetate buffer (pH 4.5) on glassy carbon electrode in the presence of common monosaccharides, disaccharides, sugar alcohol, lactate and Neu5Gc (another clinically important sialic acid) are shown in Fig. 7A and corresponding CVs are presented in Fig. S6A-P. No more than 0.8% positive bias was observed for D(+)-glucose, D(-)-fructose, D(+)-galactose, D(+)-xylose, maltose, sucrose, lactose, D(-)-xylitol, D(-)-mannitol,

D(-)-sorbitol and bovine serum albumin (BSA) even at high concentrations compared to that of Neu5Ac. However, the electrochemical responses of 1 mM Neu5Gc and lactate were found to be slightly less than that of 1 mM Neu5Ac under similar experimental conditions. A recovery analysis of 2.5 mM (expected) Neu5Ac was performed in 0.1 M acetate buffer (pH 4.5) containing 1 mM FcBA, 10 mM D(+)-glucose and 4% BSA by the standard addition method and the corresponding cathodic SWVs are shown in the inset of Fig. 7B. The overall sensitivity of the SWV decreased to 0.115 $mM^{-1}$ in the complex analytical mixture, but it was sufficient to report 2.7 mM (with 108% recovery) of Neu5Ac (Fig. 7B). The slight positive bias is due to a minor but cumulative positive interference of D(+)-glucose and 4% BSA in the overall result.

## 4. Conclusion

This preliminary work provides a proof of concept to utilise the pH sensitive formation of the more thermodynamically stable five-membered boronate ester (FcBA-1,2-β-Neu5Ac) ring of FcBA with Neu5Ac compared to other sugars, realising a simple and rapid homogeneous electrochemical assay of Neu5Ac in the linear dynamic range of 0.1-5.5 mM with a LOD of 30 μM. The present method successfully avoids interference from common monosaccharides, disaccharides and sugar alcohols, but fail to completely overcome the interference from α-hydroxy acids. Hence, it opens up a curious door to follow up investigations on the further improvisation of sensitivity and selectivity of the method, a detailed structural and in-depth energy analysis of various ester conformers by density functional theory.

## Supporting information file

Supplementary material associated with this article can be found, in the online version at

## Funding information

This project has received funding from the Enterprise Ireland and the European Union's Horizon 2020 Research and Innovation Programme under the Marie Skłodowska-Curie Career FIT PLUS grant agreement no. 847402 (Project No. MF20200140).

## CRediT authorship contribution statement

**Saurav K. Guin:** Conceptualization, Methodology, Investigation, Data curation, Visualization, Writing – original draft. **Tobias Krämer:** Supervision, Writing – review & editing. **Eithne Dempsey:** Supervision, Writing – review & editing.

## Declaration of Competing Interest

The authors declare that they have no known competing financial interests or personal relationships that could have appeared to influence the work reported in this paper.

## Data availability

Data will be made available on request.

## Acknowledgment

The authors acknowledge Dr. Fergal Lawless and Dr. Joseph Kehoe of Tirlán, Ireland. We acknowledge the Irish Centre for High-End Computing (ICHEC) for the provision of computational facilities and technical support.

## Supplementary materials

Supplementary material associated with this article can be found, in the online version, at doi:10.1016/j.electacta.2023.142618.

## References

[1] S.K. Guin, T. Velasco-Torrijos, E. Dempsey, Explorations in a galaxy of sialic acids: a review of sensing horizons, motivated by emerging biomedical and nutritional relevance, Sens. Diagn. 1 (2022) 10–70, https://doi.org/10.1039/d1sd00023c.
[2] R. Schauer, J.P. Kamerling, Exploration of the Sialic Acid World, 1st Ed., Elsevier Inc., 2018 https://doi.org/10.1016/bs.accb.2018.09.001.
[3] N. Nemanichvili, C.M. Spruit, A.J. Berends, A. Gröne, J.M. Rijks, M.H. Verheije, R. P. de Vries, Wild and domestic animals variably display Neu5Ac and Neu5Gc sialic acids, Glycobiology 32 (2022) 791–802, https://doi.org/10.1093/glycob/cwac033.
[4] F. Liu, A.B. Simpson, E. D'Costa, F.S. Bunn, S.S. van Leeuwen, Sialic acid, the secret gift for the brain, Crit. Rev. Food Sci. Nutr. (2022) 1–20, https://doi.org/10.1080/10408398.2022.2072270, 0.
[5] Y. Zhu, M. Li, Effects of sialic acid in serum and breast milk on the growth and development of infants at different stages during pregnancy and lactation, Int. J. Clin. Exp. Med. 10 (2017) 12322–12328.
[6] O.M. Sokolovskaya, M.W. Tan, D.W. Wolan, Sialic acid diversity in the human gut: molecular impacts and tools for future discovery, Curr. Opin. Struct. Biol. 75 (2022), 102397, https://doi.org/10.1016/j.sbi.2022.102397.
[7] B. Wang, J. Brand-Miller, P. McVeagh, P. Petocz, Concentration and distribution of sialic acid in human milk and infant formulas, Am. J. Clin. Nutr. 74 (2001) 510–515, https://doi.org/10.1093/ajcn/74.4.510.
[8] Z. Chen, Y. Chang, H. Liu, Y. You, Y. Liu, X. Yu, Y. Dou, D. Ma, L. Chen, X. Tong, Y. Xing, Distribution and influencing factors of the sialic acid content in the breast milk of preterm mothers at different stages, Front. Nutr. 9 (2022), 753919, https://doi.org/10.3389/fnut.2022.753919.
[9] Q. Xie, Y. Xu, W. Zhang, M. Zhu, X. Wang, J. Huang, Y. Zhuang, H. Lan, X. Chen, D. Guo, H. Li, Concentration and distribution of sialic acid in human milk and its correlation with dietary intake, Front. Nutr. 9 (2022), 929661, https://doi.org/10.3389/fnut.2022.929661.
[10] V. Andriukaitis, Commission implementing decision (EU) 2017/2375 - of 15 december 2017 - authorising the placing on the market of N-acetyl-D-neuraminic acid as a novel food ingredient under Regulation (EC) No 258/97 of the European parliament and of the council, Off. J. Eur. Union. L 337 (2017) 63–67.
[11] B. Aslan Çetin, P. Ocal, T. Irez, E. Uslu, K. Irmak, S. Karataş, The association between follicular fluid sialic acid levels, oocyte quality, and pregnancy rates, Reprod. Sci. 29 (2022) 633–638, https://doi.org/10.1007/s43032-021-00688-y.
[12] D. Liu, J. Liu, F. Ye, Y. Su, J. Cheng, Q. Zhang, Risk factors and postnatal biomarkers for acute placental inflammatory lesions and intrauterine infections in preterm infants, Eur. J. Pediatr. 181 (2022) 3429–3438, https://doi.org/10.1007/s00431-022-04545-1.
[13] G. Rizzuto, J.F. Brooks, S.T. Tuomivaara, T.I. McIntyre, S. Ma, D. Rideaux, J. Zikherman, S.J. Fisher, A. Erlebacher, Establishment of fetomaternal tolerance through glycan-mediated B cell suppression, Nature 603 (2022) 497–502, https://doi.org/10.1038/s41586-022-04471-0.
[14] J.J. Erickson, S. Archer-Hartmann, A.E. Yarawsky, J.L.C. Miller, S. Seveau, T. Y. Shao, A.L. Severance, H. Miller-Handley, Y. Wu, G. Pham, B.R. Wasik, C. R. Parrish, Y.C. Hu, J.T.Y. Lau, P. Azadi, A.B. Herr, S.S. Way, Pregnancy enables antibody protection against intracellular infection, Nature 606 (2022) 769–775, https://doi.org/10.1038/s41586-022-04816-9.
[15] M.N. Li, S.H. Qian, Z.Y. Yao, S.P. Ming, X.J. Shi, P.F. Kang, N.R. Zhang, X.J. Wang, D.S. Gao, Q. Gao, H. Zhang, H.J. Wang, Correlation of serum N-acetylneuraminic acid with the risk and prognosis of acute coronary syndrome: a prospective cohort study, BMC Cardiovasc. Disord. 20 (2020) 404, https://doi.org/10.1186/s12872-020-01690-z.
[16] L. Cheng, F. Yang, L. Tang, L. Qian, X. Chen, F. Guan, J. Zhang, G. Li, Electrochemical evaluation of tumor development via cellular interface supported CRISPR/Cas Trans-Cleavage, Research 2022 (2022), 9826484, https://doi.org/10.34133/2022/9826484.
[17] R. Sangubotla, J. Kim, Fluorometric biosensor based on boronic acid-functionalized ZnO-derived nanostructures for the detection of N-acetylneuraminic acid and its in vivo bio-imaging studies, J. Taiwan Inst. Chem. Eng. 138 (2022), 104477, https://doi.org/10.1016/j.jtice.2022.104477.
[18] R. Lin, B. Chen, D. Luo, Y. Wu, L. Huang, L. Zheng, Q. Liao, L. Huang, Molecularly imprinted polymers coated on the surface of metal–organic frameworks combined with liquid chromatography-tandem mass spectrometry for the detection of free N-acetylneuraminic acid in serum of pneumoconiosis patients, Microchem. J. 181 (2022), 107821, https://doi.org/10.1016/j.microc.2022.107821.
[19] J. Chen, N. Sun, H. Chen, Y. Zhang, X. Wang, N. Zhou, A FRET-based detection of N-acetylneuraminic acid using CdSe/ZnS quantum dot and exonuclease III-assisted recycling amplification strategy, Food Chem. 367 (2022), 130754, https://doi.org/10.1016/j.foodchem.2021.130754.
[20] J.P. Lor, J.O. Edwards, Polyol complexes and structure of the benzeneboronate ion, J. Org. Chem. 24 (1959) 769–774, https://doi.org/10.1021/jo01088a011.
[21] J.C. Norrild, H. Eggert, Evidence for mono- and bisdentate boronate complexes of glucose in the furanose form. application of 1JC-C coupling constants as a structural probe, J. Am. Chem. Soc. 117 (1995) 1479–1484, https://doi.org/10.1021/ja00110a003.

[22] S. Takahashi, N. Abiko, N. Haraguchi, H. Fujita, E. Seki, T. Ono, K. Yoshida, J. ichi Anzai, Voltammetric response of ferroceneboronic acid to diol and phenolic compounds as possible pollutants, J. Environ. Sci. 23 (2011) 1027–1032, https://doi.org/10.1016/S1001-0742(10)60509-8.
[23] H.C. Chien, T.C. Chou, A nonenzymatic amperometric method for fructosyl-valine sensing using ferroceneboronic acid, Electroanalysis 23 (2011) 402–408, https://doi.org/10.1002/elan.201000426.
[24] J.W. Tomsho, S.J. Benkovic, Elucidation of the mechanism of the reaction between phenylboronic acid and a model diol, alizarin red s, J. Org. Chem. 77 (2012) 2098–2106, https://doi.org/10.1021/jo202250d.
[25] J.S. Hansen, J.B. Christensen, J.F. Petersen, T. Hoeg-Jensen, J.C. Norrild, Arylboronic acids: A diabetic eye on glucose sensing, Sens. Actuators B Chem 161 (2012) 45–79, https://doi.org/10.1016/j.snb.2011.12.024.
[26] E. Rami Reddy, R. Trivedi, L. Giribabu, B. Sridhar, K. Pranay Kumar, M. Srinivasa Rao, A.V.S. Sarma, Carbohydrate-based ferrocenyl boronate esters: synthesis, characterization, crystal structures, and antibacterial activity, Eur. J. Inorg. Chem. (2013) 5311–5319. https://doi.org/10.1002/ejic.201300773.
[27] D. Dechtrirat, N. Gajovic-Eichelmann, F. Wojcik, L. Hartmann, F.F. Bier, F. W. Scheller, Electrochemical displacement sensor based on ferrocene boronic acid tracer and immobilized glycan for saccharide binding proteins and E. coli, Biosens. Bioelectron. 58 (2014) 1–8, https://doi.org/10.1016/j.bios.2014.02.028.
[28] K. Lawrence, T. Nishimura, P. Haffenden, J.M. Mitchels, K. Sakurai, J.S. Fossey, S. D. Bull, T.D. James, F. Marken, Pyrene-anchored boronic acid receptors on carbon nanoparticle supports: Fluxionality and pore effects, New J. Chem. 37 (2013) 1883–1888, https://doi.org/10.1039/c3nj00017f.
[29] B. Wang, S. Takahashi, X. Du, J.I. Anzai, Electrochemical biosensors based on ferroceneboronic acid and its derivatives: A review, Biosensors 4 (2014) 243–256, https://doi.org/10.3390/bios4030243.
[30] K. Lacina, M. Konhefr, J. Novotný, D. Potěšil, Z. Zdráhal, P. Skládal, Combining ferrocene, thiophene and a boronic acid: A hybrid ligand for reagentless electrochemical sensing of cis-diols, Tetrahedron Lett. 55 (2014) 3235–3238, https://doi.org/10.1016/j.tetlet.2014.04.036.
[31] A.N.J. Moore, D.D.M. Wayner, Redox switching of carbohydrate binding to ferrocene boronic acid, Can. J. Chem. 77 (1999) 681–686, https://doi.org/10.1139/v99-010.
[32] K. Lacina, P. Skládal, T.D. James, Boronic acids for sensing and other applications - a mini-review of papers published in 2013, Chem. Cent. J. 8 (2014) 1–17, https://doi.org/10.1186/s13065-014-0060-5.
[33] W. Shi, J. Wang, L. Zhu, M. Cai, X. Du, Electrochemical determination of catechin, protocatechuic acid, and L-lactic acid based on voltammetric response of ferroceneboronic acid, J. AOAC Int. 97 (2014) 1742–1745, https://doi.org/10.5740/jaoacint.13-366.
[34] M. Li, W. Zhu, F. Marken, T.D. James, Electrochemical sensing using boronic acids, Chem. Commun. 51 (2015) 14562–14573, https://doi.org/10.1039/c5cc04976h.
[35] M. Li, S.Y. Xu, A.J. Gross, J.L. Hammond, P. Estrela, J. Weber, K. Lacina, T. D. James, F. Marken, Ferrocene-boronic acid-fructose binding based on dual-plate generator-collector voltammetry and square-wave voltammetry, ChemElectroChem 2 (2015) 867–871, https://doi.org/10.1002/celc.201500016.
[36] K. Lacina, J. Novotný, Z. Moravec, P. Skládal, Interaction of ferroceneboronic acid with diols at aqueous and non-aqueous conditions - signalling and binding abilities of an electrochemical probe for saccharides, Electrochim. Acta 153 (2015) 280–286, https://doi.org/10.1016/j.electacta.2014.12.009.
[37] M. Saleem, H. Yu, L. Wang, Zain-Ul-Abdin, H. Khalid, M. Akram, N.M. Abbasi, Y. Chen, Study on synthesis of ferrocene-based boronic acid derivatives and their saccharides sensing properties, J. Electroanal. Chem. 763 (2016) 71–78, https://doi.org/10.1016/j.jelechem.2015.12.028.
[38] J. Li, Z. Bai, Y. Mao, Q. Sun, X. Ning, J. Zheng, Disposable sandwich-type electrochemical sensor for selective detection of glucose based on boronate affinity, Electroanalysis 29 (2017) 2307–2315, https://doi.org/10.1002/elan.201700295.
[39] M.A. Casulli, I. Taurino, T. Hashimoto, S. Carrara, T. Hayashita, Electrochemical assay for extremely selective recognition of fructose based on 4-ferrocene-phenylboronic acid probe and β-cyclodextrins supramolecular complex, Small 16 (2020) 1–10, https://doi.org/10.1002/smll.202003359.
[40] G.T. Williams, J.L. Kedge, J.S. Fossey, Molecular boronic acid-based saccharide sensors, ACS Sens. 6 (2021) 1508–1528, https://doi.org/10.1021/acssensors.1c00462.
[41] J.C. Norrild, I. Søtofte, Design, synthesis and structure of new potential electrochemically active boronic acid-based glucose sensorsThis work was supported by the Danish national technical research council (grant 9900690), J. Chem. Soc. Perkin Trans. 2 (2002) 303–311, https://doi.org/10.1039/b107457a.
[42] J. Yan, G. Springsteen, S. Deeter, B. Wang, The relationship among pK a, pH, and binding constants in the interactions between boronic acids and diols - It is not as simple as it appears, Tetrahedron 60 (2004) 11205–11209, https://doi.org/10.1016/j.tet.2004.08.051.
[43] L.I. Bosch, T.M. Fyles, T.D. James, Binary and ternary phenylboronic acid complexes with saccharides and Lewis bases, Tetrahedron 60 (2004) 11175–11190, https://doi.org/10.1016/j.tet.2004.08.046.
[44] K. Ishizuka, S. Takahashi, J.I. Anzai, Phenylboronic acid monolayer-modified electrodes sensitive to ribonucleosides, Electrochemistry 74 (2006) 688–690, https://doi.org/10.5796/electrochemistry.74.688.
[45] S. Liu, U. Wollenberger, M. Katterle, F.W. Scheller, Ferroceneboronic acid-based amperometric biosensor for glycated hemoglobin, Sens. Actuators, B Chem. 113 (2006) 623–629, https://doi.org/10.1016/j.snb.2005.07.011.
[46] T.D. James, M.D. Phillips, S. Shinkai, Boronic Acids in Saccharide Recognition, Royal Society of Chemistry, Cambridge, 2006.
[47] K. Lacina, P. Skládal, Ferroceneboronic acid for the electrochemical probing of interactions involving sugars, Electrochim. Acta 56 (2011) 10246–10252, https://doi.org/10.1016/j.electacta.2011.09.019.
[48] N. Katif, R.A. Harries, A.M. Kelly, J.S. Fossey, T.D. James, F. Marken, Boronic acid-facilitated α-hydroxy-carboxylate anion transfer at liquid/liquid electrode systems: the EIC rev mechanism, J. Solid State Electrochem. 13 (2009) 1475–1482, https://doi.org/10.1007/s10008-008-0709-x.
[49] F. Neese, F. Wennmohs, U. Becker, C. Riplinger, The ORCA quantum chemistry program package, J. Chem. Phys. 152 (2020), 224108, https://doi.org/10.1063/5.0004608.
[50] C. Hättig, B.A. Hess, TDMP2 calculation of dynamic multipole polarizabilities and dispersion coefficients of the noble gases Ar, Kr, Xe, and Rn, J. Phys. Chem. 100 (1996) 6243–6248, https://doi.org/10.1021/jp9528121.
[51] M. Reiher, A. Wolf, Exact decoupling of the Dirac Hamiltonian. I. General theory, J. Chem. Phys. 121 (2004) 2037–2047, https://doi.org/10.1063/1.1768160.
[52] M. Reiher, A. Wolf, Exact decoupling of the Dirac Hamlltonian. II. The generalized Douglas-Kroll-Hess transformation up to arbitrary order, J. Chem. Phys. 121 (2004) 10945–10956, https://doi.org/10.1063/1.1818681.
[53] V.N. Staroverov, G.E. Scuseria, J. Tao, J.P. Perdew, Comparative assessment of a new nonempirical density functional: Molecules and hydrogen-bonded complexes, J. Chem. Phys. 119 (2003) 12129–12137, https://doi.org/10.1063/1.1626543.
[54] J. Tao, J.P. Perdew, V.N. Staroverov, G.E. Scuseria, Climbing the density functional ladder: Nonempirical meta–generalized gradient approximation designed for molecules and solids, Phys. Rev. Lett. 91 (2003), 146401, https://doi.org/10.1103/PhysRevLett.91.146401.
[55] J.P. Perdew, J. Tao, V.N. Staroverov, G.E. Scuseria, Meta-generalized gradient approximation: Explanation of a realistic nonempirical density functional, J. Chem. Phys. 120 (2004) 6898–6911, https://doi.org/10.1063/1.1665298.
[56] F. Weigend, R. Ahlrichs, Balanced basis sets of split valence, triple zeta valence and quadruple zeta valence quality for H to Rn: Design and assessment of accuracy, Phys. Chem. Chem. Phys. 7 (2005) 3297–3305, https://doi.org/10.1039/b508541a.
[57] S. Grimme, J. Antony, S. Ehrlich, H. Krieg, A consistent and accurate ab initio parametrization of density functional dispersion correction (DFT-D) for the 94 elements H-Pu, J. Chem. Phys. 132 (2010), 154104, https://doi.org/10.1063/1.3382344.
[58] A. Allouche, Software news and updates gabedit — A graphical user interface for computational chemistry softwares, J. Comput. Chem. 32 (2012) 174–182, https://doi.org/10.1002/jcc.
[59] D.G.A. Smith, L.A. Burns, K. Patkowski, C.D. Sherrill, Revised damping parameters for the D3 dispersion correction to density functional theory, J. Phys. Chem. Lett. 7 (2016) 2197–2203, https://doi.org/10.1021/acs.jpclett.6b00780.
[60] K. Eichkorn, O. Treutler, H. Öhm, M. Häser, R. Ahlrichs, Auxiliary basis sets to approximate coulomb potentials (Chem. Phys. Letters 240 (1995) 283) (PII:0009-2614(95)00621-4), Chem. Phys. Lett. 242 (1995) 652–660, https://doi.org/10.1016/0009-2614(95)00838-U.
[61] K. Eichkorn, F. Weigend, O. Treutler, R. Ahlrichs, Auxiliary basis sets for main row atoms and transition metals and their use to approximate Coulomb potentials, Theor. Chem. Acc. 97 (1997) 119–124, https://doi.org/10.1007/s002140050244.
[62] N.B. Balabanov, K.A. Peterson, Systematically convergent basis sets for transition metals. I. All-electron correlation consistent basis sets for the 3d elements Sc-Zn, J. Chem. Phys. 123 (2005), https://doi.org/10.1063/1.1998907.
[63] D.A. Pantazis, X.Y. Chen, C.R. Landis, F. Neese, All-electron scalar relativistic basis sets for third-row transition metal atoms, J. Chem. Theory Comput. 4 (2008) 908–919, https://doi.org/10.1021/ct800047t.
[64] F. Neese, F. Wennmohs, A. Hansen, U. Becker, Efficient, approximate and parallel Hartree-Fock and hybrid DFT calculations. A "chain-of-spheres" algorithm for the Hartree-Fock exchange, Chem. Phys. 356 (2009) 98–109, https://doi.org/10.1016/j.chemphys.2008.10.036.
[65] J.D. Rolfes, F. Neese, D.A. Pantazis, All-electron scalar relativistic basis sets for the elements Rb–Xe, J. Comput. Chem. 41 (2020) 1842–1849, https://doi.org/10.1002/jcc.26355.
[66] A.V. Marenich, C.J. Cramer, D.G. Truhlar, Universal solvation model based on solute electron density and on a continuum model of the solvent defined by the bulk dielectric constant and atomic surface tensions, J. Phys. Chem. B 113 (2009) 6378–6396, https://doi.org/10.1021/jp810292n.
[67] Zhurko, G.A. Chemcraft - graphical software for visualization of quantum chemistry computations, Version 1.8, Ivanovo, 2005, https://www.chemcraftprog.com (last accessed on May 20, 2023).